In Silico Study for Acyclovir and Its Derivatives Against Mpro of nCoV: Temperature Dependent Molecular Dynamics Simulations

Madhur Singh Babu
University of Delhi
Pallavi Jain
SRMIST: SRM Institute of Science and Technology
Kamlesh Kumari
University of Delhi
Vinod Kumar
Jawaharlal Nehru University
Prashant Singh
University of Delhi
Indra Bahadur (bahadur.indra@nwu.ac.za)
North-West University

Research Article

Keywords: Molecular dynamics simulations, Molecular docking, DFT studies, ADME, Repurposing drugs, Mpro of nCoV

Posted Date: January 17th, 2022

DOI: https://doi.org/10.21203/rs.3.rs-1250241/v1

Abstract

In the present work three molecules acyclovir (A) and ganciclovir (B) are reported to cure the infection from herpes virus and others. We have designed a derivative of hydroxymethyl derivative of ganciclovir (CH_2OH of G, that is D) and investigated its potential against the Mpro of nCoV and compared with A & B. Density functional theory (DFT) calculations of A, G and D were performed using Gaussian on applying B3LYP under default condition to investigate the delocalization of electron density in their optimized geometry. Free energy of A, G and D were found to be -810.66964, -925.16575 and -1039.66047 Hartree per particle. It can be clearly seen that D have least free energy.

Further, the molecular docking of the A, B and D against the Mpro of nCoV performed using iGemdock and the binding energy for A, B and D are found to be -105.068, -110.605 and -119.226 kcal/mol. It can be clearly seen the D showed effective binding, that is maximum inhibition. For better understanding for the inhibition of the Mpro of nCoV by A, B and D, molecular dynamics simulations were performed at different temperatures, (290, 300, 310 and 320 K). Various trajectories like RMSD, RMSF, Rg and hydrogen bond were extracted and analyzed. The results of molecular docking corroborate the MD simulations that is, a better inhibitor of Mpro of nCoV.

1. Introduction

Drug repurposing is the concept of utilising an FDA- approved drug for a new problem or illness other the one for which it was originally approved. These drugs save time and money, accelerated their admittance into experimental clinical trials. The process involved the activity based on experimental or computational approach to develop the new employ of drug [1–3]. COVID-19 can cause range of illness from common cold to severe respiratory syndrome. Coronaviruses (CoV) are a family of encapsulated viruses with single-strained RNA and pathogen. In compare to previously identified SARS-CoV (2002) and MERS-CoV (2013), SARS-CoV-2 is a more virulent variant [4–7]. New SARS-CoV has recently received attention worldwide and has been declared as a public health emergency of global concern. Acyclovir is a well-known antiviral drug mostly used for the treatment of the infections due to herpes group viruse and zoster virus. A clinical research report has been published, showing the acyclovir as promising drug against the infection due to SARS-CoV-2 [8]. Heidary et al. has done the study of on acyclovir as potent molecule in COVID-19 regimens [9]. Acyclo-GTP is more efficient inhibitor of viral DNA. Ganciclovir and acyclovir have good efficacy against cytomegalovirus infection [10]. A case report had showed that ganciclovir may act as an effective antiviral drug, even against SARS-CoV-2 [11].

Molecular dynamics (MD) simulations in drug development played an important role. The behaviour of proteins and other biomolecules is captured in atomic resolution in presence or absence of small molecules. A khan et al. has performed MD simulation of anti-HIV drugs as a potent inhibitor against SARS-CoV-2 main protease [12] The electronic structure of atoms, molecules and solid can be investigated using density-functional theory (DFT) calculations. The binding affinity between the protease and ligands can be determined using iGEMDOCK 2.1 tool but it provides a preliminary information. It is used to investigate the favorable site of receptor for an effective binding of ligand [13]. There is a possibility of vander Waals interaction, hydrogen bonding between the protease and ligand. Our research group has already provided preliminary information about the docking of acyclovir and its derivatives with Mpro of nCoV [14]. A research group has done the molecular docking of acyclovir and its derivative against the main protease of SARS-CoV-2 and their binding energy are -89.64 and -96.21 kcal/mol, respectively [15]. ADME is used to know the suitability of a molecule as potent drug. ADME is used to filter the compounds to get the leading molecule from high throughput screening (HTS) campaigns.

In this work, acyclovir (A), ganciclovir, (G) and hydroxymethyl derivative of ganciclovir (D) are taken for study to inhibit the activity of main protease (Mpro) of novel corona virus (CoV) using molecular docking. Further to make the information reliable and acceptable, molecular dynamics (MD) simulations of Mpro of nCoV with designed molecules at different temperature.

2. Theoretical Calculations

2.1 Designing of ligands

Structures (acyclovir, ganciclovir and hydroxymethyl-ganciclovir) are drawn using chemdraw as in **Figure 1.**

2.2 Molecular Docking

The structure of Mpro of nCoV is downloaded from RCSB (PDB:6LU7). Before performing molecular docking, Mpro of nCoV is prepared using chimera. Structure of Mpro of nCoV was opened in chimera followed by removal of ligand and atoms were deleted and the structure was saved in PDB format [16–18]. All three ligands structures were optimized by applying MM2 forcefield on chemdraw 3D before molecular docking. The docking was performed using iGEMDOCK 2.1 and gives binding energy in kcal/mol [19].

2.3 DFT Calculation

DFT calculation of A, G and D were performed by using Gaussian 16.0 and Gaussview 6 as an interface [20, 21]. The parameter applied to perform calculation are optimization plus frequency with B3LYP and the basis set was 6-311G at 298 K.

2.4 Molecular dynamics (MD) simulations

Temperature dependent MD simulation of Mpro of nCoV with A, G and D were performed at 290, 300, 310 and 320 K by using online the web server WebGro (https://simlab.uams.edu/) and it uses GROMACS to perform the calculations [22–26]. Input parameter used are as ; forcefield GROMACS9643a, box type triclinic, water model is SPC and salt type is NaCl. Equilibration and MD run parameter used pressure (1bar), number of frames per simulation 1000 and simulation time (100ns). The GlycoBioChem PRODRG2 is an online server was used (http://davapc1.bioch.dundee.ac.uk/cgi-bin/prodrg) used to create topology of small molecules [27].

2.5 Absorption, Distribution, Metabolism and Excretion (ADME) of A, G and D

A molecule may be a drug if it has the ability to reach its target location with sufficient concentration and active in the body for the timespan of biological response. In this work, a free web tool swissADME (http://www.swissadme.ch) has been used to predict the different physiochemical and pharmacokinetics property of A, G and D.

3. Result And Discussion

3.1 Molecular docking of A, D ang G

Molecular docking is technique used to characterize the protein-ligand interaction using computational tools like autodock, paradock, iGEMDOCK method. Docked poses were given in the two and three-dimensional view to visualize the molecular interaction. 3D views mainly focused on the conventional Hydrogen bonding while the 2D view focused on the all-possible interactions like non-conventional hydrogen bonding, hydrophobic interaction, electrostatic, etc. Docking analysis shows that A forms five classical hydrogen bonding with PHE-140 (2.76), GLU-166 (3.19, 2.10, 2.86) and with CYS-145 (2.90), D forms eight conventional hydrogen bonds with GLY-143, (2.05) SER-144 (2.99), CYS-145 (2.37), HIS-163 (2.87), HIS-164 (2.90), ASP-187 (3.25), TYR-54 (2.88, 2,76), G forms six hydrogen bonds with HIS-164 2.58, HIS-163 (2.84), GLY-143 (2.32), SER-144 (2.65), CYS-145 (2.23, 3.12). Analysis of non-conventional hydrogen bonding A form bonds with HIS-163 (2.45), D form bonds with GLY-143 (2.89) and G form bonds with ARG-188 (2.41), MET-165 (2.21), HIS-41 (3.3), ASP-187 (3.02). Hydrophobic interactions were also analyzed for ligand because it helps to stabilize the ligands into the active binding cavity of protein. A shows hydrophobic interaction with MET-165 (2.54), D with CYS-145 (4.10) and G with MET-49 (4.25, 5.46) and MET-165 (5.10).

Table 1
shows the binding energy of different dock poses of acyclovir, ganciclovir and hydroxymethyl-ganciclovir.

S.No	Ligand	Total Energy	Ligand	Total Energy	Ligand	Total Energy
1	A-0	-104.785	G-0	-109.324	D-0	-118.124
2	A -1	-103.521	G-1	-110.567	D-1	-118
3	A -2	-104.53	G-2	-107.279	D-2	-112.417
4	A-3	-103.388	G-3	-110.605	D-3	-113.368
5	A-4	-103.05	G-4	-109.548	D-4	-119.226
6	A-5	-103.917	G-5	-109.292	D-5	-113.106
7	A-6	-105.054	G-6	-109.132	D-6	-114.796
8	A-7	-105.068	G-7	-108.602	D-7	-116.265
9	A-8	-104.73	G-8	-107.609	D-8	-114.076
10	A-9	-103.084	G-9	-107.915	D-9	-109.424

Table 2
Different types of interaction of A, G and D with Mpro of nCoV.

Ligand	H-Bond				Hydrophobic	
	Classical		**Non-classical**			
	Amino Acid	**Distance**	**Amino Acid**	**Distance**	**Amino Acid**	**Distance**
A	PHE-140	2.60	HIS-163	2.37	MET-165	2.50
	GLU-166	2.05, 2.70, 3.22				
	CYS-145	2.96				
G	ASN-142	3.10, 3.32	HIS-172	1.76		
	SER-144	2.67	MET-165	2.91		
	CYS-145	1.79	HIS-41	2.74		
D	SER-144	2.43	GLY-143	2.54		
	ASN-142	3.18	HIS-172	1.62		
	HIS-41	2.80	ASN-142	3.68		
			HIS-163	2.99		
			HIS-41	3.05		

3.2 DFT calculations

Different thermodynamic parameters such as enthalpy, free energy, optimization energy, thermal energy and zero-point energy were calculated. HOMO can serve as an electron donor [28] and LUMO is the first can act as an electron acceptor [29]. Higher the energy of HOMO indicate more the ability to donate electron density. HUMO, LUMO and optimized geometry of A, G and D are given in **Figure 3.**

Further, different thermodynamics parameter such as zero-point Energy, thermal energy, Optimization energy and thermal enthalpy are calculated and no significant changes is found as in Table 3. Free energies are an important parameter for deciding the stability of compound. It is considered that lesser the free energy of molecule indicates higher stability. Among A, G and D, D has the least free energy -1039.7090 (Hartree per particle) and considered to more stable. Dipole moment is also an important parameter for predicting the solubility in aqueous medium. Table 3 shows that G has the highest dipole moment of 10.4241a.u. in all.

Table 3
Thermodynamic parameters of A, G and D.

Compound	Sum of electronic and zero-point Energies (Hartree per particle)	Sum of electronic and thermal Energies (Hartree per particle)	Sum of electronic and thermal Enthalpies (Hartree per particle)	Sum of electronic and thermal Free Energies (Hartree per particle)	Optimization energy (Hartree per particle)	Dipole moment (a.u.)
A	-810.66964	-810.65477	-810.65382	-810.65382	-810.880213	9.7791
G	-925.16575	-925.14840	-925.14746	-925.21332	-925.40877	10.4241
D	-1039.66047	-1039.6412	-1039.64026	-1039.7090	-1039.93684	8.9611

Various physiochemical descriptors were also determined for above reported three molecules by DFT calculation as given **Table in 4**. E_{LUMO} and E_{HOMO} are significant chemical factors for determining a molecules reactivity and are also applied to derive a range of important chemical reactivity descriptors such as chemical hardness (), chemical potential (μ), softness(S), electronegativity (χ) are reported in Table 4. Energy gap of HOMO and LUMO is a useful parameter for determining the reactivity of compound. The HOMO and LUMO energy are directly proportional to the ionization potential and electron affinity.

Table 4
Physio-chemical descriptors of acyclovir, ganciclovir and hydroxymethyl-ganciclovir

S.No.	Compound	E_{LUMO}	E_{HOMO}	$E_{HOMO-LUMO}$	$E_{LUMO+HOMO}$		χ	S	μ	Ω
1	A	-0.0297	-0.2252	-0.1955	-0.2549	-0.0978	0.12745	-5.1154	-0.1275	-0.0831
2	D	-0.0297	-0.2251	-0.1953	-0.2548	-0.0977	0.12740	-5.1201	-0.127	-0.0831
3	G	-0.0294	-0.2245	-0.1951	-0.2538	-0.0975	0.12692	-5.1264	-0.1269	-0.0826

3.3 Molecular dynamics simulations

Molecular dynamics simulations is used to analyze the dynamic of macromolecular system. It uses the trajectories obtained from MD simulations and gives useful information to investigate the protein-ligand interactions [30, 31]. MD simulations main protease of nCoV with of A, G and D were performed for 100 ns at different temperature. Root mean square deviation is the measure of the average of square root of deviation from the mean distance [32, 33]. It provides the conformational stability of macromolecular system due to binding of ligand into binding cavity. RMSD values ranges between the 0.2 nm to 0.5 nm. It was also found that on increasing temperature the RMSD value increases. Lower temperature favors stabilization of protein-ligand complex. During simulations, no loop was seen which indicates less deviation due to binding of the ligands Figure 4.

Root mean square fluctuation is used to study the fluctuation values of the atomic coordinates of the atoms of amino acids [34]. Fluctuations values were used to analyze the configurational changes in the presences of ligand at different temperature. RMSF graphs for the protein with A, G and D were analyzed and given the Figure 5. From the analysis, fluctuations were recorded in range of 140-160, 40-60, 160-180, 240-260 amino acids. Most of the fluctuations were occur in the range of amino acid comes in molecular docking range.

Radius of gyration is the measure of the distance between center of mass and axis of rotation. It is used to study the stability of protein in presence of small molecules. Lesser the value of radius of gyration indicates higher the stability [35, 36]. Radius of gyration values were analyzed for the main protease of nCoV in presence of A, G and D at different temperature (Figure 6). At low temperature, radius of gyration is less meaning more stability. But an increasing temperature value of Rg increases and thus the stability decreases. Results of molecular docking corroborate the results obtained by MD simulations.

Molecular dynamic simulation analysis used to examine their of Mpro of nCoV in presence of A, G and D over time span at various temperature. Conventional hydrogen bonding is more significant and formed between fluorine, oxygen and nitrogen with hydrogen. The anchoring is tighter as the number of hydrogen bond increases and the length of hydrogen bond decreases [37, 38]. The number of hydrogen bonds and their persistency were analyzed during simulation at different temperatures as given in Figure 7. Maximum number of hydrogen bonds were found 6 in case of acyclovir while in case of derivative and ganciclovir maximum hydrogen bonds are five.

3.4 Absorption, Distribution, Metabolism and Excretion (ADME) of A, G and D

ADME characteristics is as important in the drug development process [39]. ADME drug characteristics such as absorption, distribution, metabolism and elimination are critical to a drug candidate's clinical success. It is estimated that about 50% of the drugs fails due to insufficient effectiveness which includes low bioavailability due to inadequate intestinal absorption and poor metabolic stability [40–43]. Lipophilicity is one of the most important criteria to predict the molecule as a drug and it is a partition coefficient of n-octanol and water (log $P_{O/W}$). It determines the amount of solute dissolves in the water v/s organic solvent in a solution [44]. The partition coefficient is a significant indicator of a substance physical constitution and determines its behavior in various situation. For effective drug, the value of log $P_{O/W}$ is less than or equal to 5 [45]. Solubility is an important criterion for deciding a molecule to be drug, therefore, log S should be less than 6. According to Lipinski's rule of five an orally active drug must have: (i) hydrogen bond donor less than or equal to five (ii) hydrogen bond acceptor less than or equal to ten (iii) molecular mass less than 500g/mol (iv) log P values less than 5 [46–48]. Table 5 shows the physiochemical properties of A, G and D. All the studied molecules obey the Lipinski rule of 5.

Table 5
Physiochemical properties of acyclovir, ganciclovir and hydroxymethyl-ganciclovir

Physiochemical properties	Acyclovir	Ganciclovir	Derivative of acyclovir
Log S	-0.41	-0.42	0.37
Solubility	Very soluble	Very soluble	Highly soluble
Heavy atoms	16	18	20
Molecular weight (g/mol)	225.20	255.23	285.26
No. of rotational bonds	4	**5**	**6**
No. H-bond acceptors	5	6	**7**
Num. H-bond donors	**3**	4	**5**
Log $P_{o/w}$ (WLOGP)	-1.48	-2.11	-2.75
Physiochemical space for oral bioavailability	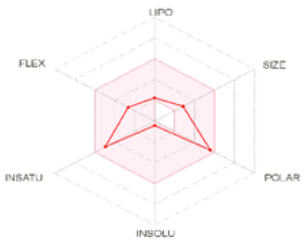	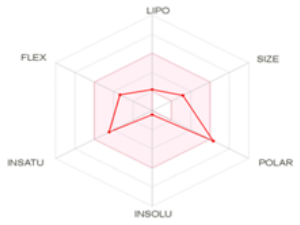	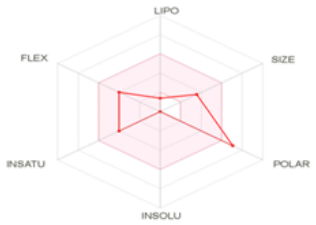

Drug likeness is an important criterion for evaluating behavior of molecule during early stage of drug development. This factor may be regarded as a way to link physicochemical properties of a compound to its biopharmaceutical properties in the human body for oral delivery. Despite the fact that there are several methods for delivery of oral dosages is favored for patient comfort and compliance. At various stages of the discovery process, early assessment of oral bioavailability i.e. the percentage of the dosage that reaches the blood following oral administration, is a significant decision- making factor. Bioavailability is influenced by a number of factors but gastrointestinal absorption is most important. The BBB may be regarded as a shield that protects the brain through a “physical” barrier and a “biochemical” barrier (e.g. P glycoprotein pumping out substrate from CNS tissues). Blood-brain barrier is a system that ensure the consistency of central nervous system environment by allowing brain tissues to interchange nutrient with the outside world. Effective BBB penetration is important for targeting CNS illness, but non-CNS drugs should have restricted BBB penetration due to side effect [49]. Despite the importance of active transport, passive diffusion is the primary route for drug to reach the brain from the blood. The method for assessing active efflux through biological membrane such as from the gastrointestinal wall to the lumen or from the brain, requires knowledge of compounds that are substrate or non- substrate of the permeability glycoprotein. P-gp has a number of functions, one of which is to protect the central nervous system from xenobiotics. TPSA is a key characteristic for drug likeness and its value must be smaller than 130 Å. TPSA is considered to be a useful indicator of a compounds ability to transport drug. In Table 6 bioactivity and drug likeness score of A, G and D are given. A shows high GI absorption, TPSA value 119.06 Å and following Lipinski rule with zero violation [50, 51]. G and D have TPSA value more than 130 Å but they followed the Lipinski rule with zero violation.

Table 6
Bioactivity and Drug likeness score of acyclovir, ganciclovir and hydroxymethyl-ganciclovir

C. No.	GI absorption	BBB permeant	Lipinski rule	Log K_p (skin permeation) (cm/s)	TPSA (Å)	P-gp substrate
A	High	No	Yes; 0 violation	-8.78	119.06	No
G	Low	No	Yes; 0 violation	-9.04	139.29	No
D	Low	No	Yes; 0 violation	-10.20	159.52	No

4. Conclusion

Herein, author have taken the repurposing drugs (acyclovir, ganciclovir and derivative of ganciclovir) and docked it against with Mpro of nCoV using iGEMDOCK. The binding energy of A, Gr and D are -105.068, -110.65 and -119.226 kcal/mol respectively. D has minimum binding energy of -119.226 kcal/mol, means it may be a promising inhibitor of Mpro of nCoV. For more reliable data authors have performed temperature dependent MD simulation of Mpro of nCoV with A, G and D using WebGro at 290, 300, 310 and 320 K. MD simulations corroborates with docking results. Further DFT calculation of A, G and D are performed using Gaussian 16 to see the localization of electron density and stability. Result shows that D has minimum free energy of -1039.7090 Hartree per particle. Further, ADME properties of A, G and D were calculated using swissADME to evaluate solubility, bioavailability and potential of molecule to become effective drug. It has been found that A, G and D followed the Lipinski rule with no violation and falls in acceptable range for their bioavailability.

Declarations

Funding There is source of financial support to perform the work.

Disclosure of potential conflicts of interest and informed consent: I further confirm that the order of authors listed in the manuscript has been approved by all of us. The authors have relevant financial and non-financial interests to disclose.

Availability of data and material: *"The datasets generated during and/or analysed during the current study are available from the corresponding author on reasonable request."*

Code availability: N/A

Authors' contributions: *"All authors contributed to the study conception and design. Material preparation, data collection and analysis were performed by [*Madhur Singh Babu*], and [Pallavi Jain]. The first draft of the manuscript was written by [Prahsant Singh], [Vinod Kumar] and [Kamlesh Kumari]. All authors read and approved the final manuscript."*

Research involving Human Participants and/or Animals It is declared that no human participants and/or animals are used in this work.

References

1. Phadke M, Saunik S (2020) COVID-19 treatment by repurposing drugs until the vaccine is in sight. Drug Dev Res 81:541–543. https://doi.org/https://doi.org/10.1002/ddr.21666
2. Schlagenhauf P, Grobusch MP, Maier JD, Gautret P (2020) Repurposing antimalarials and other drugs for COVID-19, Travel Med. Infect Dis 34:101658. https://doi.org/10.1016/j.tmaid.2020.101658
3. Deftereos SN, Andronis C, Friedla EJ, Persidis A, Persidis A (2011) Drug repurposing and adverse event prediction using high-throughput literature analysis. WIREs Syst Biol Med 3:323–334. https://doi.org/https://doi.org/10.1002/wsbm.147

4. Mann R, Perisetti A, Gajendran M, Gandhi Z, Umapathy C, Goyal H (2020) Clinical Characteristics, Diagnosis, and Treatment of Major Coronavirus Outbreaks. Front Med 7:766. https://doi.org/10.3389/fmed.2020.581521
5. Nassar A, Ibrahim IM, Amin FG, Magdy M, Elgharib AM, Azzam EB, Nasser F, Yousry K, Shamkh IM, Mahdy SM, Elfiky AA, A Review of Human Coronaviruses' Receptors: The Host-Cell Targets for the Crown Bearing Viruses, Molecules 26 (2021). https://doi.org/10.3390/molecules26216455
6. Rahimi A, Mirzazadeh A, Tavakolpour S (2021) Genetics and genomics of SARS-CoV-2: A review of the literature with the special focus on genetic diversity and SARS-CoV-2 genome detection. Genomics 113:1221–1232. https://doi.org/https://doi.org/10.1016/j.ygeno.2020.09.059
7. Naqvi AAT, Fatima K, Mohammad T, Fatima U, Singh IK, Singh A, Atif SM, Hariprasad G, Hasan GM, Hassan MI (2020) Insights into SARS-CoV-2 genome, structure, evolution, pathogenesis and therapies: Structural genomics approach, Biochim. Biophys Acta Mol Basis Dis 1866:165878. https://doi.org/10.1016/j.bbadis.2020.165878
8. Baker VS (2021) Acyclovir for SARS-CoV-2: An ClinicalPractice old drug with a new purpose. Clin Pract 18:1584–1592
9. Heidary F, Madani S, Gharebaghi R, Asadi-amoli F (2021) Acyclovir as a Potential Add-on Therapy in COVID-19 Treatment Regimens. Pharm Sci 27:S68–S77. https://doi.org/10.34172/PS.2021.38
10. Weller DR, Balfour HH Jr, Vezina HE (2009) Simultaneous determination of acyclovir, ganciclovir, and (R)-9-[4-hydroxy-2-(hydroxymethyl)butyl]guanine in human plasma using high-performance liquid chromatography. Biomed Chromatogr 23:822–827. https://doi.org/10.1002/bmc.1192
11. Ben Salem M, Salima L, Mouna H, Taieb SK, Handous I, Manel BS, Ahmed LS, Sabra AS, Skhiri H, Immunosuppressive drugs and ganciclovir: two modalities to prevent COVID-19 severity: a case report, PAMJ Clin Med 5 (2021). https://doi.org/10.11604/pamj-cm.2021.5.86.28901
12. Khan A, Ali SS, Khan MT, Saleem S, Ali A, Suleman M, Babar Z, Shafiq A, Khan M, Wei D-Q (2021) Combined drug repurposing and virtual screening strategies with molecular dynamics simulation identified potent inhibitors for SARS-CoV-2 main protease (3CLpro). J Biomol Struct Dyn 39:4659–4670. https://doi.org/10.1080/07391102.2020.1779128
13. Kumar MP, Sundaram KM, Ramasamy MS, Coronavirus spike (S) glycoprotein (2019-ncov) targeted siddha medicin es kabasura kudineer and thonthasura kudineer–in silico evidence for c orona viral drug, Asian J. Pharm. Res. Heal. Care. 12 (n.d.) 20–27
14. Kumar D, Sanatan AR, Kumari K, Bahadur I, Singh P, Promising Acyclovir and its derivatives to inhibit the protease of SARS-CoV-2: Molecular Docking and Molecular Dynamics simulations, (2020) 1–17
15. Arunkumar B, Fernandez A, Laila SP, Nair AS (2020) Molecular Docking Study of Acyclovir and Its Derivatives As Potent Inhibitors in Novel Covid-19. Int J Pharm Sci Res 11:4700. https://doi.org/10.13040/IJPSR.0975-8232.11(9).4700-05
16. Bender BJ, Gahbauer S, Luttens A, Lyu J, Webb CM, Stein RM, Fink EA, Balius TE, Carlsson J, Irwin JJ, Shoichet BK (2021) A practical guide to large-scale docking. Nat Protoc 16:4799–4832. https://doi.org/10.1038/s41596-021-00597-z
17. Ugbe FA, Shallangwa GA, Uzairu A, Abdulkadir I (2021) Activity modeling, molecular docking and pharmacokinetic studies of some boron-pleuromutilins as anti-wolbachia agents with potential for treatment of filarial diseases. Chem Data Collect 36:100783. https://doi.org/https://doi.org/10.1016/j.cdc.2021.100783
18. Burley SK, Berman HM, Kleywegt GJ, Markley JL, Nakamura H, Velankar S, Protein Data Bank (PDB) (2017) The Single Global Macromolecular Structure Archive. In: Wlodawer A, Dauter Z, Jaskolski M (eds) Protein Crystallogr. Methods Protoc. Springer New York, New York, pp 627–641. https://doi.org/10.1007/978-1-4939-7000-1_26
19. Hsu K-C, Chen Y-F, Lin S-R, Yang J-M (2011) iGEMDOCK: a graphical environment of enhancing GEMDOCK using pharmacological interactions and post-screening analysis. BMC Bioinformatics 12:S33. https://doi.org/10.1186/1471-2105-12-S1-S33
20. Frisch MJ, Trucks GW, Schlegel HB, Scuseria GE, Robb MA, Cheeseman JR, Scalmani G, Barone V, Petersson GA, Nakatsuji H, Li X, Caricato M, Marenich AV, Bloino J, Janesko BG, Gomperts R, Mennucci B, Hratchian HP, Ortiz JV, Izmaylov AF, Sonnenberg JL, Williams-Young D, Ding F, Lipparini F, Egidi F, Goings J, Peng B, Petrone A, Henderson T, Ranasinghe D, Zakrzewski VG, Gao J, Rega N, Zheng G, Liang W, Hada M, Ehara M, Toyota K, Fukuda R, Hasegawa J, Ishida M, Nakajima T, Honda Y, Kitao O, Nakai H, Vreven T, Throssell K, Montgomery JA Jr, Peralta JE, Ogliaro F, Bearpark MJ, Heyd JJ, Brothers

EN, Kudin KN, Staroverov VN, Keith TA, Kobayashi R, Normand J, Raghavachari K, Rendell AP, Burant JC, Iyengar SS, Tomasi J, Cossi M, Millam JM, Klene M, Adamo C, Cammi R, Ochterski JW, Martin RL, Morokuma K, Farkas O, J.B. Foresman, D.J. Fox, Gaussian 16, Rev. C.01, Gaussian 16, Rev. C. 01. (2016)

21. Dennington R, Keith TA, Millam JM, GaussView Version 6, n.d
22. BEKKER H, BERENDSEN HJC, DIJKSTRA EJ, ACHTEROP S, VONDRUMEN R, VANDERSPOEL D, SIJBERS A, Keegstra H, RENARDUS MKR, GROMACS - A PARALLEL COMPUTER FOR MOLECULAR-DYNAMICS SIMULATIONS, in: DeGroot RA, Nadrchal J (eds), World Scientific Publishing, n.d.: pp. 252–256
23. Abraham MJ, Murtola T, Schulz R, Páll S, Smith JC, Hess B, Lindah E, Gromacs: High performance molecular simulations through multi-level parallelism from laptops to supercomputers, SoftwareX. 1–2 (2015) https://doi.org/10.1016/j.softx.2015.06.001
24. Lindorff-Larsen K, Piana S, Palmo K, Maragakis P, Klepeis JL, Dror RO, Shaw DE, Improved side-chain torsion potentials for the Amber ff99SB protein force field, Proteins Struct. Funct Bioinforma 78 (2010). https://doi.org/10.1002/prot.22711
25. Lindahl E, Bjelkmar P, Larsson P, Cuendet MA, Hess B, Implementation of the charmm force field in GROMACS: Analysis of protein stability effects from correction maps, virtual interaction sites, and water models, J Chem Theory Comput 6 (2010). https://doi.org/10.1021/ct900549r
26. Oostenbrink C, Villa A, Mark AE, Van Gunsteren WF, A biomolecular force field based on the free enthalpy of hydration and solvation: The GROMOS force-field parameter sets 53A5 and 53A6, J Comput Chem 25 (2004). https://doi.org/10.1002/jcc.20090
27. Schüttelkopf AW, van Aalten DMF (2004) {\it PRODRG}: a tool for high-throughput crystallography of protein{–}ligand complexes. Acta Crystallogr Sect D 60:1355–1363. https://doi.org/10.1107/S0907444904011679
28. Singh MB, Kumar A, Jain P, Singh P, Kumari K, An insight of novel eutectic mixture between thiazolidine-2,4-dione and zinc chloride: Temperature-dependent density functional theory approach, J. Phys. Org. Chem. n/a (n.d.) e4305. https://doi.org/https://doi.org/10.1002/poc.4305
29. Song S, Kim M-C, Sim E, Benali A, Heinonen O, Burke K, Complexes (2018) Benchmarks and Reliable DFT Results for Spin Gaps of Small Ligand Fe(II). J Chem Theory Comput 14:2304–2311. https://doi.org/10.1021/acs.jctc.7b01196
30. Chen Z, Yi J, Zhao H, Luan H, Xu M, Zhang L, Feng D (2021) Strength development and deterioration mechanisms of foamed asphalt cold recycled mixture based on MD simulation. Constr Build Mater 269:121324. https://doi.org/https://doi.org/10.1016/j.conbuildmat.2020.121324
31. Shukla R, Tripathi T, Molecular Dynamics Simulation of Protein and Protein–Ligand Complexes BT - Computer-Aided Drug Design, in: D.B. Singh (Ed.), Springer Singapore, Singapore, 2020: pp. 133–161. https://doi.org/10.1007/978-981-15-6815-2_7
32. Aier I, Varadwaj PK, Raj U (2016) Structural insights into conformational stability of both wild-type and mutant EZH2 receptor. Sci Rep 6:34984. https://doi.org/10.1038/srep34984
33. Schreiner W, Karch R, Knapp B, Ilieva N, Relaxation Estimation of RMSD in Molecular Dynamics Immunosimulations, Comput. Math. Methods Med (2012) (2012) 173521. https://doi.org/10.1155/2012/173521
34. Sargsyan K, Grauffel C, Lim C (2017) How Molecular Size Impacts RMSD Applications in Molecular Dynamics Simulations. J Chem Theory Comput 13:1518–1524. https://doi.org/10.1021/acs.jctc.7b00028
35. Justino GC, Nascimento CP, Justino MC (2021) Molecular dynamics simulations and analysis for bioinformatics undergraduate students. Biochem Mol Biol Educ 49:570–582. https://doi.org/https://doi.org/10.1002/bmb.21512
36. Zhu J, Lv Y, Han X, Xu D, Han W (2017) Understanding the differences of the ligand binding/unbinding pathways between phosphorylated and non-phosphorylated ARH1 using molecular dynamics simulations. Sci Rep 7:12439. https://doi.org/10.1038/s41598-017-12031-0
37. Chikalov I, Yao P, Moshkov M, Latombe J-C (2011) Learning probabilistic models of hydrogen bond stability from molecular dynamics simulation trajectories. BMC Bioinformatics 12:S34. https://doi.org/10.1186/1471-2105-12-S1-S34

38. Sessions RB, Gibbs N, Dempsey CE (1998) Hydrogen Bonding in Helical Polypeptides from Molecular Dynamics Simulations and Amide Hydrogen Exchange Analysis: Alamethicin and Melittin in Methanol. Biophys J 74:138–152. https://doi.org/https://doi.org/10.1016/S0006-3495(98)77775-6
39. Cannady E, Katyayan K, Patel N (2022) Chapter 3 - ADME Principles in Small Molecule Drug Discovery and Development: An Industrial Perspective. In: Haschek WM, Rousseaux CG, Wallig MA, Bolon B (eds) Haschek Rousseaux's Handb. Toxicol. Pathol. (Fourth Ed., Fourth Edi. Academic Press, pp 51–76. https://doi.org/https://doi.org/10.1016/B978-0-12-821044-4.00003-0
40. Prueksaritanont T, Tang C (2012) ADME of Biologics—What Have We Learned from Small Molecules? AAPS J 14:410–419. https://doi.org/10.1208/s12248-012-9353-6
41. Daina A, Michielin O, Zoete V (2017) SwissADME: a free web tool to evaluate pharmacokinetics, drug-likeness and medicinal chemistry friendliness of small molecules. Sci Rep 7:42717. https://doi.org/10.1038/srep42717
42. Daina A, Zoete V, A BOILED-Egg To Predict Gastrointestinal Absorption and Brain Penetration of Small Molecules, ChemMedChem. 11 (2016) 1117–1121. https://doi.org/https://doi.org/10.1002/cmdc.201600182
43. Daina A, Michielin O, Zoete V, iLOGP (2014) A Simple, Robust, and Efficient Description of n-Octanol/Water Partition Coefficient for Drug Design Using the GB/SA Approach. J Chem Inf Model 54:3284–3301. https://doi.org/10.1021/ci500467k
44. Özkan H, Adem Ş, Synthesis, Spectroscopic Characterizations of Novel Norcantharimides, Their ADME Properties and Docking Studies Against COVID-19 Mpr°, ChemistrySelect. 5 (2020) 5422–5428. https://doi.org/https://doi.org/10.1002/slct.202001123
45. Deb S, Reeves AA, Hopefl R, Bejusca R, ADME and Pharmacokinetic Properties of Remdesivir: Its Drug Interaction Potential, Pharmaceuticals 14 (2021). https://doi.org/10.3390/ph14070655
46. Ghose AK, Viswanadhan VN, Wendoloski JJ (1999) A Knowledge-Based Approach in Designing Combinatorial or Medicinal Chemistry Libraries for Drug Discovery. 1. A Qualitative and Quantitative Characterization of Known Drug Databases. J Comb Chem 1:55–68. https://doi.org/10.1021/cc9800071
47. Egan WJ, Merz Kenneth M, Baldwin JJ (2000) Prediction of Drug Absorption Using Multivariate Statistics. J Med Chem 43:3867–3877. https://doi.org/10.1021/jm000292e
48. Lipinski CA, Lombardo F, Dominy BW, Feeney PJ (1997) Experimental and computational approaches to estimate solubility and permeability in drug discovery and development settings. Adv Drug Deliv Rev 23:3–25. https://doi.org/https://doi.org/10.1016/S0169-409X(96)00423-1
49. Terasaki T (2017) Quantitative expression of ADME proteins at the blood-brain barrier. Drug Metab Pharmacokinet 32:S12. https://doi.org/https://doi.org/10.1016/j.dmpk.2016.10.059
50. Sawamoto T, Haruta S, Kurosaki Y, Higaki K, Kimura T (1997) Prediction of the Plasma Concentration Profiles of Orally Administered Drugs in Rats on the Basis of Gastrointestinal Transit Kinetics and Absorbability. J Pharm Pharmacol 49:450–457. https://doi.org/10.1111/j.2042-7158.1997.tb06823.x
51. Kimura T, Higaki K, Transit G, Absorption D (2002) Biol Pharm Bull 25:149–164. https://doi.org/10.1248/bpb.25.149

Figures

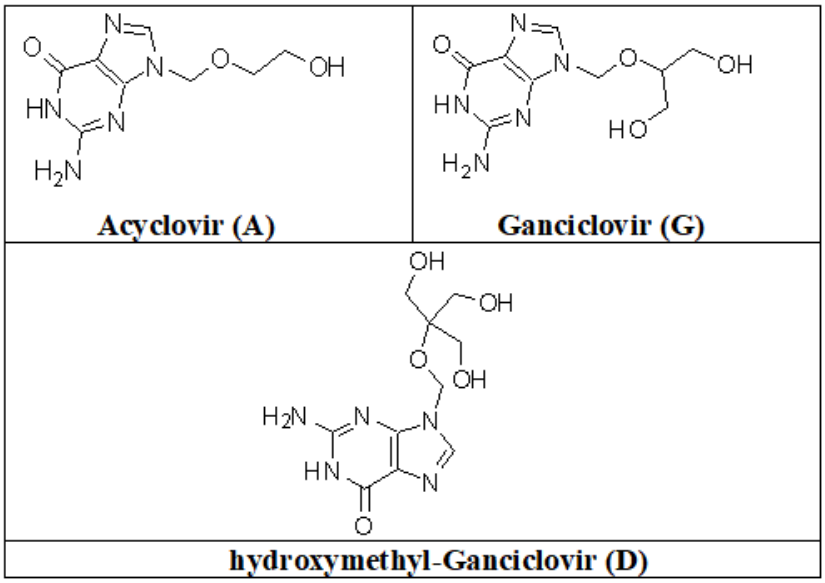

Figure 1

Structures of A, G and D.

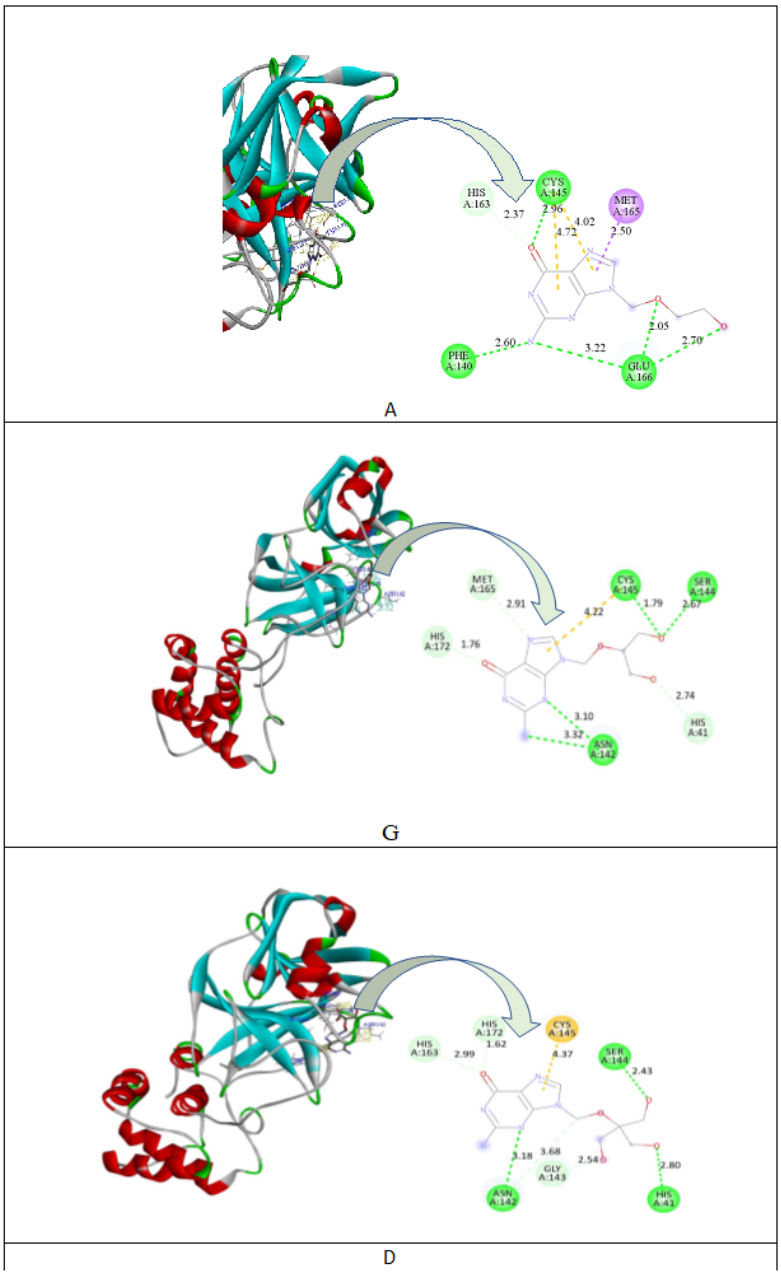

Figure 2

Three dimensional and two-dimensional dock view of A, G and D with Mpro of nCoV.

C.No.	HOMO	LUMO	Optimized geometry
TEMPERATURE 298 K			
A	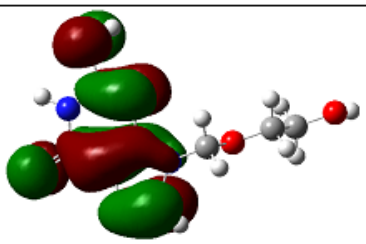	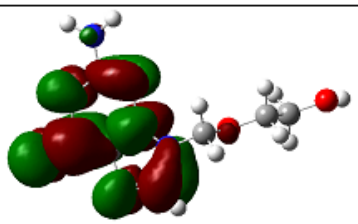	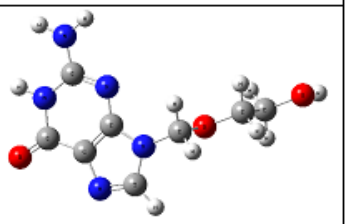
G	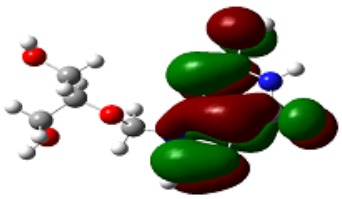	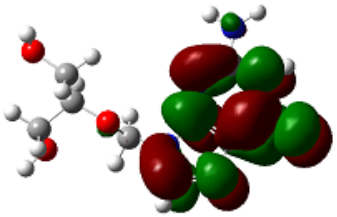	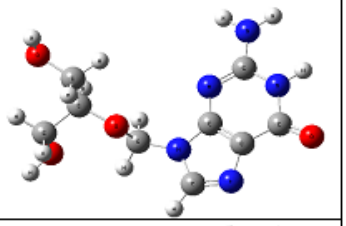
D	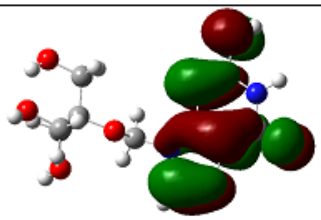	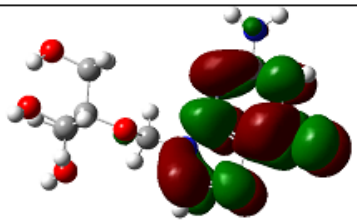	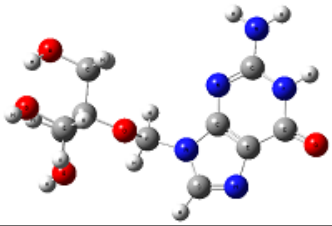

Figure 3

HOMO, LUMO and Optimized geometry structures of A, G and D.

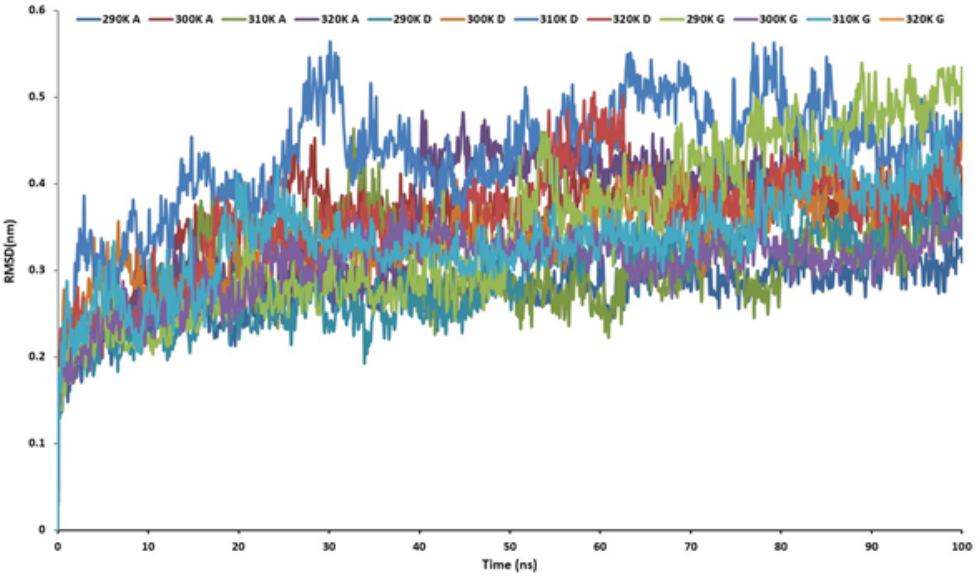

Figure 4

Trajectory of RMSD fit to backbone for the Mpro of nCoV with A, G and D at 290, 300, 310 and 320 K.

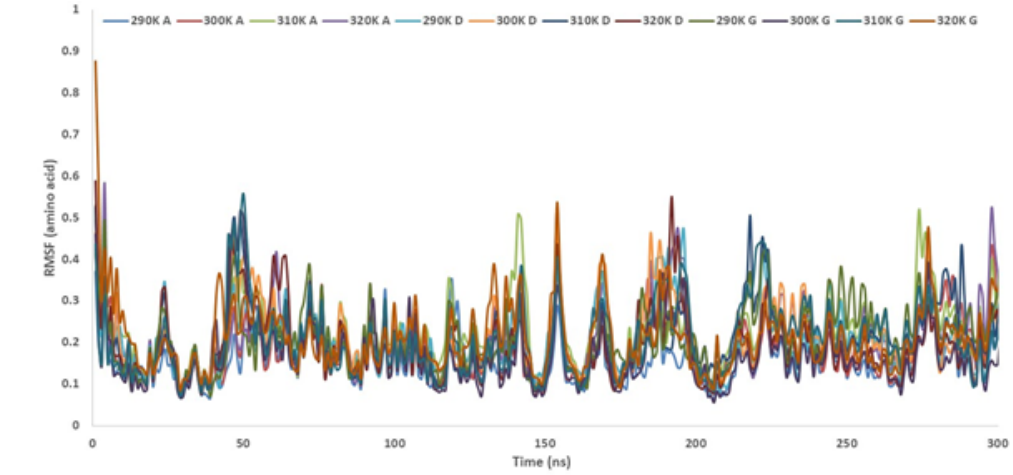

Figure 5

Trajectory of RMSF for the Mpro of nCoV with A, G and D at 290, 300, 310 and 320 K.

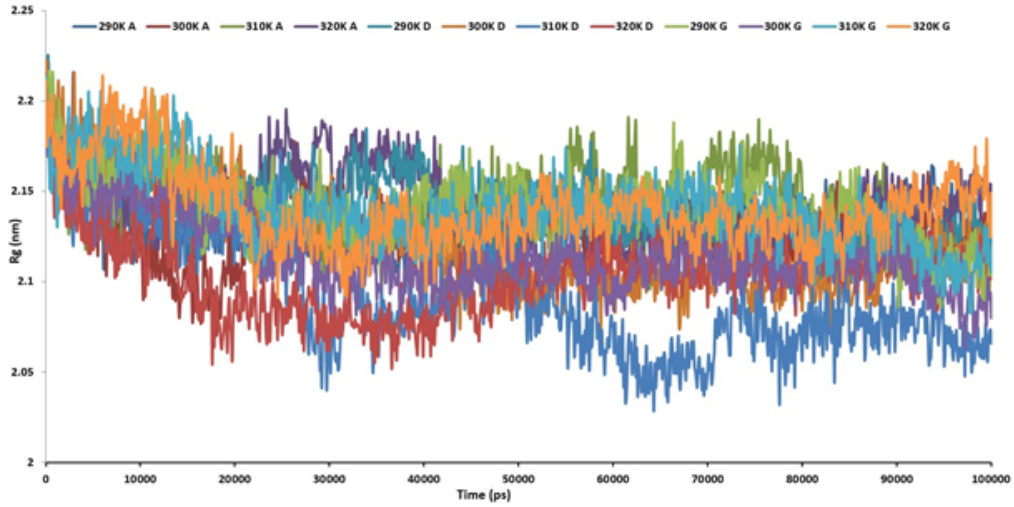

Figure 6

Trajectory of radius of gyration for the Mpro of nCoV with A, G and D at 290, 300, 310 and 320 K.

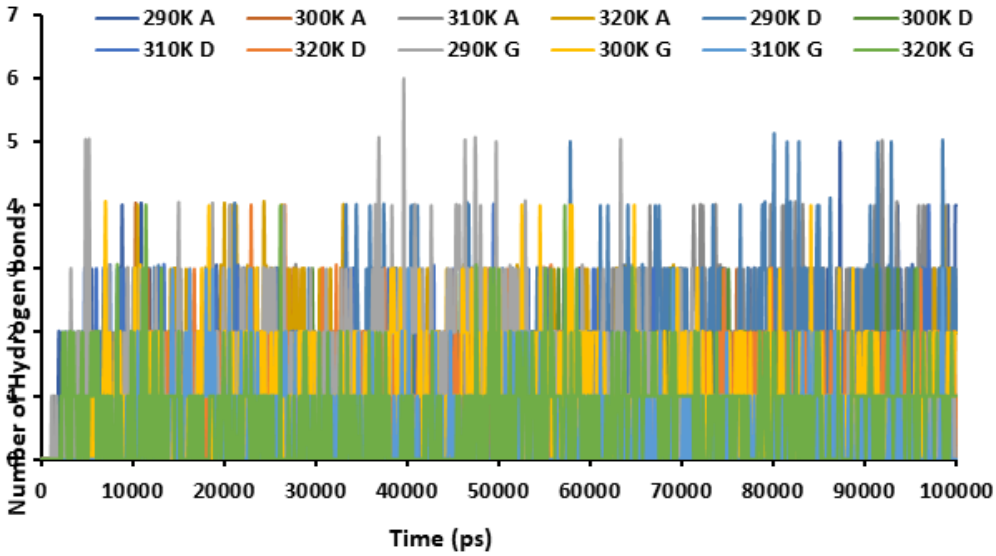

Figure 7

Trajectory of H-bond for the Mpro of nCoV with A, G D at 290, 300, 310 and 320 K.